Nature Environment and Pollution Technology
An International Quarterly Scientific Journal

p-ISSN: 0972-6268
(Print copies up to 2016)
e-ISSN: 2395-3454

Vol. 25 | No. 1 | Article ID D1801 | 2026

Original Research Paper

https://doi.org/10.46488/NEPT.2026.v25i01.D1801

Open Access Journal

Bacterial Diversity in Oil Field Environments and Evaluation of Their Ability to Biosynthesize Silver Nanoparticles (AgNPs)

Alaa H. Hamel[1], Wijdan H. Al-Tamimi[2]† and Murtadha H. Fayadh[1]
[1]Department of Biology, College of Education for Pure Sciences, University of Basrah, Basrah 61004, Iraq
[2]Department of Biology, College of Science, University of Basrah, Basrah 61004, Iraq
†Corresponding author: Wijdan H. Al-Tamimi; wijdan.abdulsahib@uobasrah.edu.iq

Abbreviation: Nat. Env. & Poll. Technol.
Website: www.neptjournal.com

Received: 24-04-2025
Revised: 06-06-2025
Accepted: 10-06-2025

Key Words:

Oil field environment
Universal 16SrDNA gene
Silver nanoparticles synthesis

ABSTRACT

Bacteria isolated from oil reservoir environments possess unique enzymes that allow them to adapt to extreme environments, making them ideal candidates for producing high-value nanomaterials that can be used in various fields. In the present study, eight samples were collected from Badra and Ahdab oil fields in Iraq, the bacteria isolated and identified based on the *16SrRNA* gene, and the isolates were screened for the synthesis of silver nanoparticles (AgNPs). The characteristics of the AgNPs were analyzed using UV-Vis spectroscopy, FTIR, XRD, FE-SEM, zeta potential measurements, and dynamic light scattering (DLS). The results indicated the dominance of Gram-positive bacteria, with a percentage of 18 (72%). Genetic identification revealed that the bacteria were under 6 genera and 16 species; these genera include *Enterococcus*, *Priestia*, *Enterobacter*, *Acinetobacter*, *Flavobacterium*, and *Bacillus*. Seven new strains have been deposited in GenBank. The results of screening isolates for synthesized AgNPs showed high efficiency of a novel strain, *Bacillus halotolerans* strain AhWM4, with the maximum absorption peak at 430 nm. The average size of AgNPs using XRD, FE-SEM, and TEM was (31.3, 27.0, and 42.1) nm, respectively. Dynamic light scattering (DLS) measurements showed a wide dispersion with an effective diameter of 57.1 nm; the X-ray diffraction (XRD) spectrum matched the crystalline nature of the AgNPs. It also showed high stability, with a zeta potential of -42.3 mV. AgNPs have attracted considerable attention due to their staggering potential for a wide range of commercial and environmental applications.

Citation for the Paper:

Hamel, A.H., Al-Tamimi, W.H. and Fayadh, M.H., 2026. Bacterial diversity in oil field environments and evaluation of their ability to biosynthesize silver nanoparticles (AgNPs). *Nature Environment and Pollution Technology*, 25(1), D1801. https://doi.org/10.46488/NEPT.2026.v25i01.D1801

Note: From 2025, the journal has adopted the use of Article IDs in citations instead of traditional consecutive page numbers. Each article is now given individual page ranges starting from page 1.

INTRODUCTION

The biosynthesis of silver nanoparticles (AgNPs) has been explored in various environments, but using bacteria isolated from harsh conditions such as oil reservoirs-characterised by a lack of oxygen, high temperatures, and extreme pressures-represents a significant innovation. These extreme environments challenge most forms of life and provide new insights into how microorganisms may enhance industrial processes, particularly in nanotechnology production. In 1926, Bastin discovered sulphur-reducing bacteria such as Desulfoplanes, Desulfovermiculus, and Desulfotignum within harsh environments (Kadnikov et al. 2023). The study of microbial communities in oil reservoir environments has since opened a new chapter in our understanding of these ecosystems. Subsequent research has revealed diverse microorganisms inhabiting oil reservoirs, including those found in crude oil, formation water, rocks, and organic matter, particularly in the oil–water transition zone (OWTZ), which is conducive to microbial growth and oil decomposition (Rajbongshi and Gogoi 2021).

The positive effects of these microbial communities can be harnessed by investigating their activities, metabolic processes, and capacity to produce bioproducts such as surfactants, biopolymers, solvents, acids, and gases (Augustine 2023). Much current research focuses on oil-contaminated environments, where

Alishewanella jeotgali, Bacillus cereus, and Pseudomonas stutzeri have likely adapted to harsh conditions and developed significant enzyme systems of interest for both environmental and commercial applications (AL-assdy et al. 2024, AL-Shami et al. 2023, Alyousif et al. 2022, Aboud et al. 2021, Hamzah et al. 2020a). Among these applications, the biosynthesis of AgNPs is gaining attention due to its environmentally friendly, energy-efficient, cost-effective, and rapid nature compared with traditional physical and chemical methods (Yali et al. 2023).

Furthermore, AgNPs have diverse applications in medicine, food technology, and environmental science (Arshad et al. 2024). The degradation of mixed polluted compounds such as oil spills, heavy metals, herbicides, particulate matter, pesticides, fertilisers, toxic gases, sewage, and industrial effluents (Singh et al. 2020) can be performed effectively using nanocatalysts (Astruc 2020). Recent studies indicate a direct relationship between nitrate reduction by microorganisms and their ability to synthesise AgNPs. Evidence suggests that the biological reduction of nitrate may release free electrons, which can subsequently reduce silver ions (Ag^+) to form AgNPs. This mechanism highlights the capacity of bacteria to transform toxic metals into non-toxic nanoforms and produce AgNPs with unique properties (Rose et al. 2023). The connection between nitrate reduction and nanoparticle synthesis underscores the importance of studying this process to better understand the biological mechanisms involved in AgNP biosynthesis.

Nanoparticles can be produced by extracellular or intracellular bacteria, often involving organic molecules such as proteins, sugars, and enzymes, which are believed to be crucial in reducing metal ions and forming nanoparticles through oxidation–reduction reactions (John et al. 2022). Despite significant advances in nanoparticle biosynthesis, gaps remain in our understanding of how microorganisms convert metals into nanoparticles, particularly in oilfield environments (Bharose et al. 2024). Characterising the bacterial community structure of produced water from oil fields presents significant challenges, including the difficulty of cultivating bacteria using conventional methods, which rely mainly on culture-based approaches rather than molecular analyses (Ziganshina et al. 2023). Therefore, DNA sequencing approaches, particularly targeting the 16S rRNA gene, have greatly enhanced our understanding of these microbial communities and their composition (Gao et al. 2024).

Research has revealed a remarkable diversity of bacterial species inhabiting oil reservoirs, with hundreds recorded and several species identified for their high capacity to produce

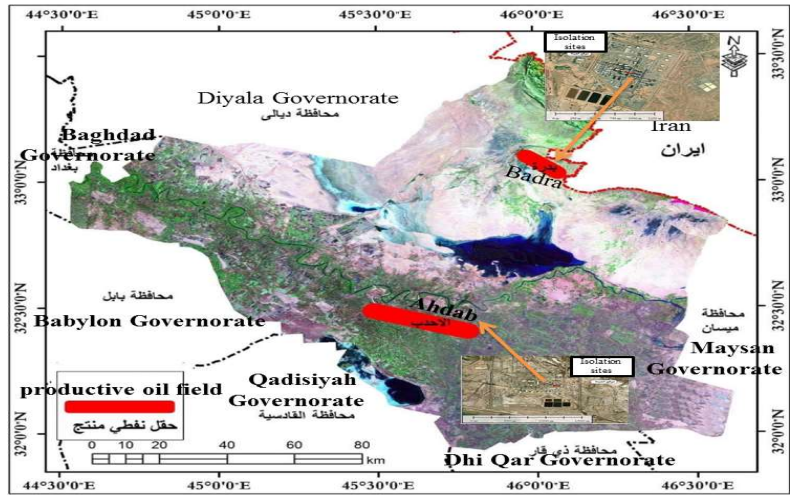

Fig. 1: Sample collection sites.

Table 1: Physicochemical properties of the produced water samples obtained from Badra and Ahdab oil fields.

Samples	Oil in water ppm	TSS ppm	pH	Total Iron ppm	Hydrogen sulfide ppm	Chloride ppm
BD- s 1	85	20.0	6.6	0.69	371.96	21423
BD- s 2	92	15.0	6.8	0.78	400	19080
Ah- s1	36.94	37.0	6.85	0.10	406	130804.81
Ah- s2	34.15	42.0	6.87	0.10	377	143362.65

BD = Badra, Ah = Ahdab, s = sites, TSS = Total Suspended Solids

AgNPs, paving the way for new insights in biological research and nanotechnology. In the Badra and Ahdab oil fields, the existence of bacterial communities has not yet been explored, and no data are available. Hence, the present study aims to isolate and identify bacteria from the reservoirs of these oil fields in Wasit Governorate, Iraq, and determine the most efficient isolates for synthesising AgNPs, while characterising the produced nanoparticles using different techniques.

MATERIALS AND METHODS

Sample Collection

Eight samples of produced water were collected from separator tanks of the Badra and Ahdab oil fields between October and December 2022. The Badra oil field is located in the northeast of Wasit Governorate in Iraq at approximately 33.037°N and 46.056°E. The depth of oil reservoirs was between 4700 and 6200 m below ground, depending on primary production of oil, while in the Ahdab oil field, located to the west of Wasit at approximately 32.424°N and 45.714°E, the oil reservoirs were between 2300 and 3500 m deep, extracting oil through flooding with water for secondary production Fig. 1. The samples were collected in sterile glass containers and transported to the laboratory immediately, keep at room temperature until used. Daily reports from the oil field laboratories were used to determine the physical and chemical properties of the samples Table 1.

Culturing of Bacteria

To isolate the indigenous bacteria, 5mL of each sample was inoculated into a 250mL Erlenmeyer flask containing 95 mL of nutrient broth. The flasks were incubated in a shaker at 35°C and 120 rpm for 48 h After the incubation period, 1 mL from each flask was serially diluted and spread using an L-shaped glass spreader onto the center of sterilized nutrient agar and MacConkey agar plates and incubated aerobically at 35°C for 24 h. Distinct colonies were isolated, and the subculture process was conducted three times to ensure the purity of the colonies. Additionally, the Gram stain protocol was employed for microscopic analysis.

Molecular Identification of Bacteria

Each isolate was activated for 24 h at 35°C in nutrient broth medium. An Eppendorf tube containing 1.5 ml of culture was centrifuged for two minutes at 13,000 rpm. After discarding the supernatant, DNA was extracted from the cells by the Presto™ Mini gDNA kit according to the manufacturer's instructions (Geneaid, Taiwan). A 1% agarose gel was used to prove the extracted gene. Identification of the isolated bacteria was performed using a 1500-bp-long *16S rRNA* gene. Polymerase chain reaction (PCR) was used for amplification, using the universal forward primer 27F 5'-AGAGTTTGATCCTGGCTCAG-3' and the reverse primer 1492R 5'GGTTACCTTGTTACGACTTR-3'. The AccuPower® PCR PreMix kit prepares the reaction mixture according to the manufacturer's instructions. The program of the thermal cycle was as follows: initial denaturation at 95°C for 5min., followed by denaturation with 30 cycles of 95°C for 30 sec., primer annealing at 52°C for 45sec., extension at 72°C for 1.5min., and final extension at 72°C for 10 min. (Alyousif et al. 2020). To verify the amplification of the target gene, the fragment of amplified DNA was separated using an electrophoresis device on a 1.5% (w/v) agarose gel stained with 0.5 µl of ethidium bromide to a concentration of 0.5 µg/mL (Lee et al. 2012). The amplified and labeled DNA tubes were sent to Macrogen Laboratories in South Korea for sequence analysis. The results were compared with the NCBI website using BLAST to identify the closest matches to the bacterial isolate. The phylogenetic tree was constructed using the neighbor-joining (NJ) technique in MEGA 11, with 1000 primers incorporated to ensure robustness (Burghal et al. 2021).

Screening the Ability of Bacterial Isolates to Synthesize AgNPs

All bacterial isolates were screened for the synthesis of AgNPs by the nitrate reduction test, which was conducted according to Bhusal & Muriana (2021). The positive isolates were selected for screened on nutrient agar supplemented with 1 mM $AgNO_3$, and the bacterial isolates were inoculated on the plates, incubated at 35°C for 24 to 72 h. The growth of bacteria indicated a positive result; the isolates that gave a positive result were chosen for the final screening, which was carried out to select the most efficient isolates for synthesizing AgNPs, based on changes in the color of the reaction mixture, following the method described by Bhusal & Muriana (2021) with some modifications. Selected bacterial strains were cultured in a 250 mL Erlenmeyer flask, incubated in a shaker at 35°C with a speed of 180 rpm for 24 h. After incubation, the cultures were centrifuged at 6000 rpm for 20 min. The resulting supernatant was then filtered using a Millipore filter with a pore diameter of 0.45 µm. Next, the reaction mixture was prepared by mixing equal volumes 1:1 (v/v) of the supernatant and a 1mM $AgNO_3$ solution in an aluminum-coated flask to prevent oxidation. The mixture was then incubated in a shaker at 180 rpm and 35°C for 72 to 120 h. The results were evaluated by observing the color change of the reaction mixture from yellow to dark brown compared with the control (nutrient broth with $AgNO_3$ solution). After the incubation period, to confirm the presence of AgNPs in

the reaction mixture, 2 mL of each mixture that had changed color to brown was taken and poured into a quartz cuvette. The absorbance was measured in the range of (200-800) nm using the UV-1800 double-beam spectrophotometer (Shimadzu, Japan).

Purification of AgNPs

After measuring the absorbance, the reaction mixture that achieved the highest absorbance peak was placed in test tubes in a centrifuge at 6000 rpm for 20 min, the supernatant was discarded, and the remaining precipitate was washed with deionized distilled water. This step was repeated three times until a clear and colorless solution was obtained. In the final step of centrifugation, the precipitate containing AgNPs was placed in a clean watch glass in an electric oven at 50°C to dry and remove excess water. The resulting powder was then collected in Eppendorf tubes covered with aluminum foil (AL-Shami et al. 2023).

Characterization of AgNPs Synthesized

The *Bacillus halotolerans* strain AhWM4 that gave the highest peak in the UV-visible spectrophotometer was characterized by an infrared spectrometer (Shimadzu, Japan). An X-ray diffractometer (PANalytical, Netherlands) is employed to ascertain the crystalline characteristics of AgNPs and to compute their size utilizing the Debye-Scherrer equation (Saleh & Alwan 2020). The detailed structure of the AgNPs was studied using a field emission scanning electron microscope (FE-SEM) and transmission electron microscope (TEM) (Hitachi, Japan), while the elemental composition was determined with energy dispersive X-ray spectroscopy (EDX). A zeta potential device (HORIBA Scientific SZ-100, Japan) was used to assess the surface charges of AgNPs, and dynamic light scattering (DLS) was employed to analyze the particle size and distribution in the colloidal solutions (Pallavi et al. 2022).

RESULTS AND DISCUSSION

Isolation of Bacteria

Twenty-five strains were isolated from the produced water of the Badra and Ahdab oil fields. 15 (60%) isolates from the Badra oil field and 10 (40%) from Ahdab, according to the protocol of Gram stain. In the Badra oil field, 4 (26.7%) isolates were Gram-negative, and 11 (73.3%) were Gram-positive, while in Ahdab, the numbers of Gram-negative and positive isolates were 3 (30%) and 7 (70%), respectively, as Fig. 2.

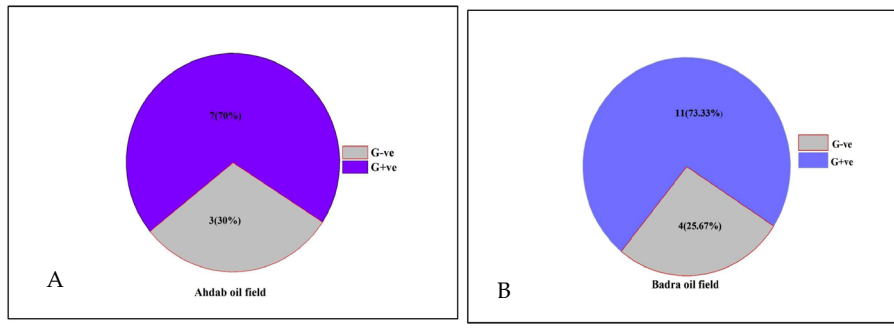

Fig. 2: Total percentage of Gram-positive and Gram-negative bacteria in produced water samples, A Ahdab oil field and B Badra oil field.

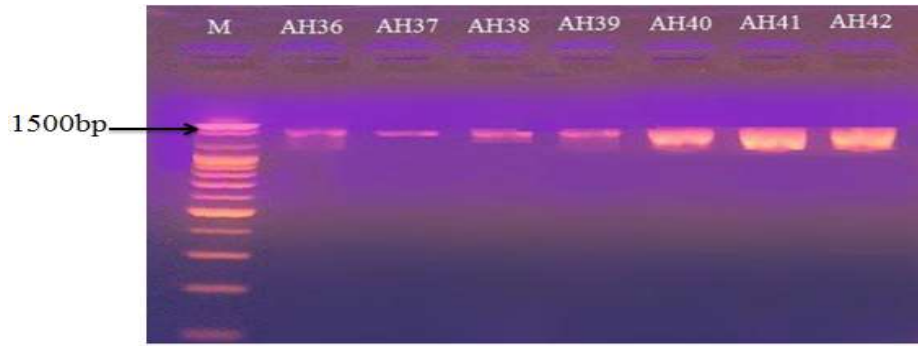

Fig. 3: Electrophoretic analysis demonstrating the amplified *16S rRNA* gene products derived from genomic DNA of some bacterial isolates. M. Ladder, AH36-AH42 AH code of bacterial isolates.

Table 2: Bacterial community of produced water samples that were identified by the *16S rRNA* gene (Ah Isolation symbol before molecular identification, BD= Badra oil field, Ah= Ahdab oil field).

Site	Accession no. reference strain	Isolates code	Cloest species	Match ratio with reference strain %
BD- s1	AH42	OM033656.1	Enterobacter hormaechei	100 %
	AH45	MN208152.1	*Enterobacter cloacae*	100 %
	AH14	OP852942.1	*Bacillus paramycoides*	98 %
	AH38	MN049561.1	*Acinetobacter calcoaceticus*	99 %
	AH36	KX950679.1	*Bacillus cereus strain MBGIPS 9*	100 %
	AH37	MN847602.1	*Bacillus velezensis*	99 %
	AH31	KF051091.1	*Flavobacterium columnare*	100 %
	AH18	FJ573187.1	*Bacillus cereus strain AK1871*	100 %
BD- s2	AH46	MT000148.1	*Enterococcus faecium*	100 %
	AH19	KY362201.1	*Bacillus amyloliquefaciens*	99 %
	AH30	KC790242.1	Bacillus anthracis	100 %
	AH11	MK547152.1	Bacillus tropicus	100 %
	AH10	MZ618716.1	Bacillus subtilis	100 %
	AH21	ON510000.1	Bacillus anthracis	100 %
	AH20	KR999903.1	Priestia flexa	99 %
Ah- s1	AH47	MN658825.1	*Enterobacter hormaechei*	100 %
	AH39	OP288194.1	*Enterobacter hormaechei*	100 %
	AH41	MT783973.1	*Bacillus cereus*	100 %
	AH40	MH050744.1	*Enterobacter cloacae*	100 %
Ah- s2	AH4	OK298998.1	*Bacillus rugosus*	99 %
	AH5	OQ152470.1	*Bacillus toyonensis*	100 %
	AH15	KX268482.1	*Bacillus cereus*	100 %
	AH3	MT539995.1	*Bacillus subtilis*	100 %
	AH12	LK392517.1	*Bacillus cereus strain ISU-02*	%100
	AH13	MT539148.1	*Bacillus halotolerans*	99 %

Genetic Identification of Bacterial Isolates

The *16S rRNA* gene was amplified to identify the bacterial isolates using the polymerase chain reaction (PCR) technique. Agarose gels 1% (w/v) displaying PCR-amplified 16S rDNA gene fragments. About 1,500 bp of amplified fragments were obtained for every isolate, determined based on the DNA marker (100 bp) (Fig. 3).

The BLAST tool was used to analyze and compare the DNA sequencing results of the bacterial isolates with those of the reference strains found in the GenBank database. The DNA sequencing results of most of the studied strains showed a 100% similarity in gene sequences compared to the reference strains, as shown in Table 2. However, some isolated strains displayed variations in certain nitrogenous bases relative to the reference strains available in GenBank. Seven new strains were recorded in the GenBank database, with unique accession numbers as illustrated in Table 3.

Table 3: The new bacterial strains that were deposited in the NCBI GenBank database

Name of the new strain in GenBank	Accession no.
Bacillus paramycoides strain AhWM5	PP559174.1
Acinetobacter calcoaceticus strain AWMBI11	PP564426.1
Bacillus velezensis strain AWMBI10	PP564424.1
Bacillus amyloliquefaciens strain AhWM6	PP559314.1
Priestia flexa strain AhWM7	PP559502.1
Bacillus rugosus strain AhWM2	PP558901.1
Bacillus halotolerans strain AhWM4	PP559020.1

The results of the phylogenetic tree also confirmed a clear genetic proximity between the studied isolates and the reference strains, as shown in Fig. 4.

DNA sequencing of the bacterial community of produced water samples revealed that bacterial isolates were under six different bacterial genera and belonged to sixteen species. The genera were *Enterococcus*, *Priestia, Enterobacter, Acinetobacter, Flavobacterium, and Bacillus*. Among them, the genus Bacillus was the most prevalent, 16 (64%), followed by *Enterobacter*, 5 (20%). For the species, *Bacillus cereus* was the most frequently recorded, 5 (20%), followed by *Enterobacter hormaechei*, 3 (12%) (Fig. 5).

Screening of Bacterial Isolates for the Ability to Synthesize AgNPs

All bacterial isolates were tested for the synthesis of AgNPs. The screening results by the nitrate reductase enzyme test showed that 18 of the isolates gave positive results. Only these isolates were screened on nutrient agar supplemented with 1mM $AgNO_3$, and the results revealed that only 11

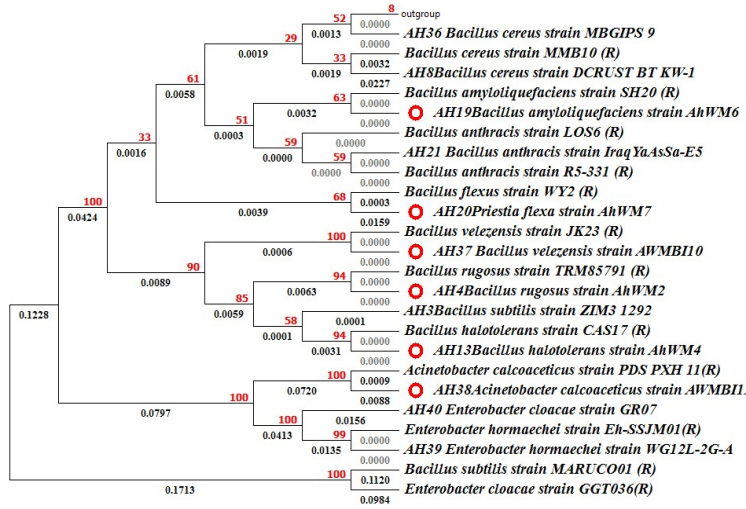

Fig. 4: A phylogenetic tree that shows the evolutionary relationships among bacterial strains of different species and their reference strains (R).

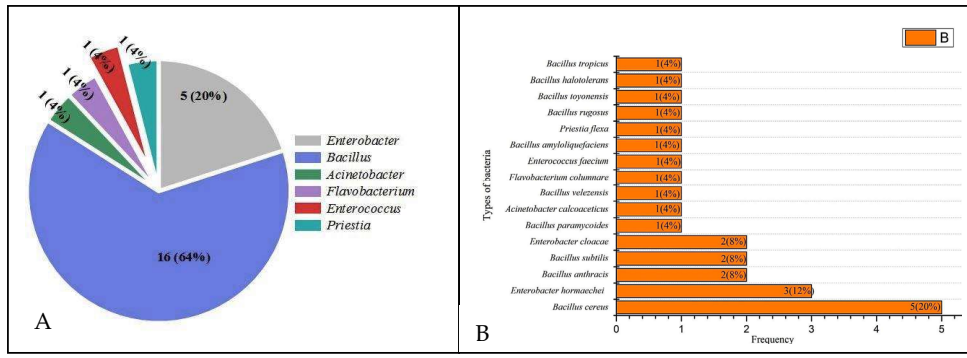

Fig. 5: Frequency of bacterial isolates in samples. (A). Percentage of genera (B). Percentage of species.

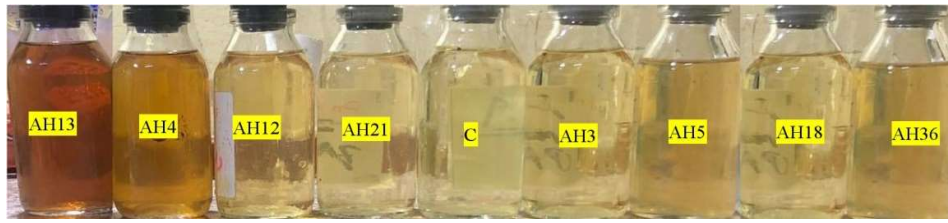

Fig. 6: Screening of bacterial isolates based on color change of the mixture: (AH). Isolates. (C). Control.

showed growth. These isolates were tested for a color change, as the supernatant of bacterial cultures treated with 1 mM $AgNO_3$. Only 2 strains, *Bacillus halotolerans* strain AhWM4 and *Bacillus rugosus* strain AhWM2, showed extracellular formation of AgNPs, which was initially validated by observing the color change of the supernatants from light yellow to brown compared to the control after the incubation period, indicating the formation of AgNPs (Fig. 6).

The UV-vis spectrophotometer was used to detect the biosynthesis of AgNPs after the color change of the mixture reaction of two strains, AH 13 and AH 4. *Bacillus halotolerans* strain AhWM4 and *Bacillus rugosus* strain AhWM2. The results indicated a maximum absorption peak of 0.47 λmax at 430 nm and 0.09 λmax at a wavelength of 440 nm, using the supernatant for both strains, respectively, indicating the synthesis of AgNPs with different optical properties (Fig. 7).

Characterization of AgNPs Synthesized by *Bacillus halotolerans* Strain AhWM4

Fourier transform infrared spectroscopy (FTIR): The FTIR spectra were used to identify the various functional groups of the synthesized AgNPs by Bacillus halotolerans strain AhWM4 that contributed to stability and the reduction of precursors to NPs. The results displayed peaks at specific wavelengths, specifically around 13495, 12935, and 1552 cm^{-1}. These peaks correspond to O-H stretching from hydrogen-bonded alcohols and phenolic vibrations, as well as C-H bonds in alkanes and C=O bonds in carbonaceous compounds, ketones, aldehydes, and carboxylic acids. N-H bonds in amides and secondary amines. The results further indicated a shift and a decrease in the intensity of some bands in the spectrum of the AgNPs formed during the reduction process. Notably, the peaks at 3214.19 cm^{-1}, 1647.21 cm^{-1}, and 1554.86 cm^{-1} showed a decrease in intensity and a shift in position (Fig. 8).

The X-ray diffraction (XRD) analysis: The crystallinity of AgNPs synthesized by the B. halotolerans strain AhWM4 was examined using XRD analysis. Five distinct diffraction peaks were observed at 2θ values of 38.27˚, 45.94˚, 55.59˚, 67.42˚, and 76.94˚. These peaks correspond to the silver crystal planes (200, 103, 006, 112, and 201), closely matching the previously cited reference (JCPDS: 00-041-1402). Additionally, the X-ray diffraction (XRD) pattern exhibited three extra peaks at 2θ values of 27.83˚, 32.32˚, and 57.61˚, which could be associated with the crude coating agents (Fig. 9). According to Scherrer's the average crystallite size of the AgNPs was calculated to be 31.3 nm.

Electron microscopy (FE-SEM): According to the Field Emission Scanning Electron Microscopy (FE-SEM) and Transmission Electron Microscopy (TEM) images, the particles synthesized by the B. halotolerans strain AhWM4 were spherical or sub-spherical and exhibited a polydisperse nature. The average sizes of the nanoparticles were between 27.0 nm and 42.1 nm, respectively, with no signs of agglomeration (Fig. 10).

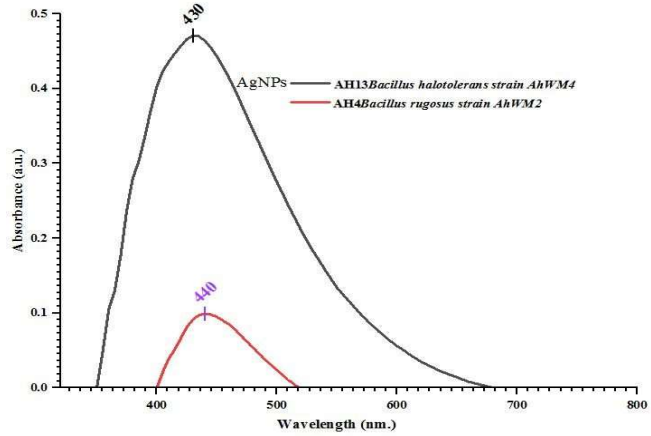

Fig. 7: UV-vis spectra of AgNPs biosynthesized by bacterial strains after color change in the reaction mixture.

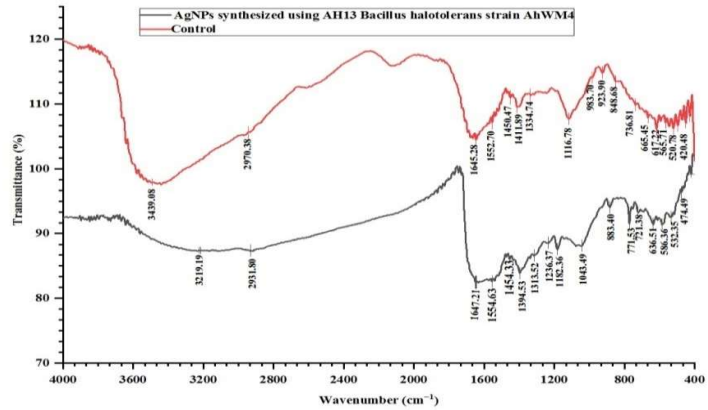

Fig. 8: FTIR spectra of control and Ag NPs synthesized by *B. halotolerans* strain AhWM4.

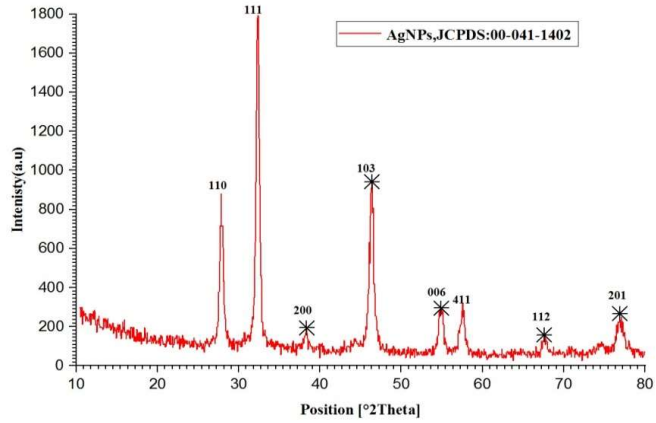

Fig. 9: XRD spectra of AgNPs synthesized by *B. halotolerans* strain AhWM4.

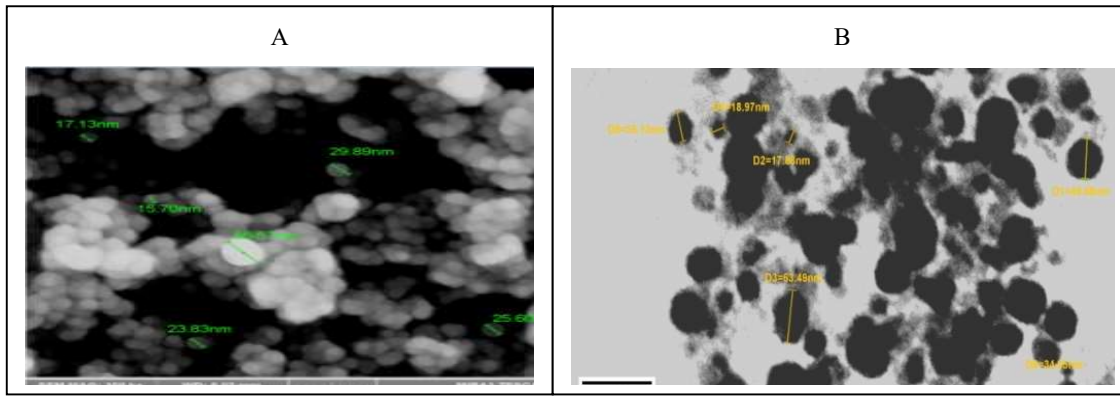

Fig. 10: Characteristic of AgNPs synthesized using *B. halotolerans* strain AhWM4: (A). FE-SEM (B). TEM.

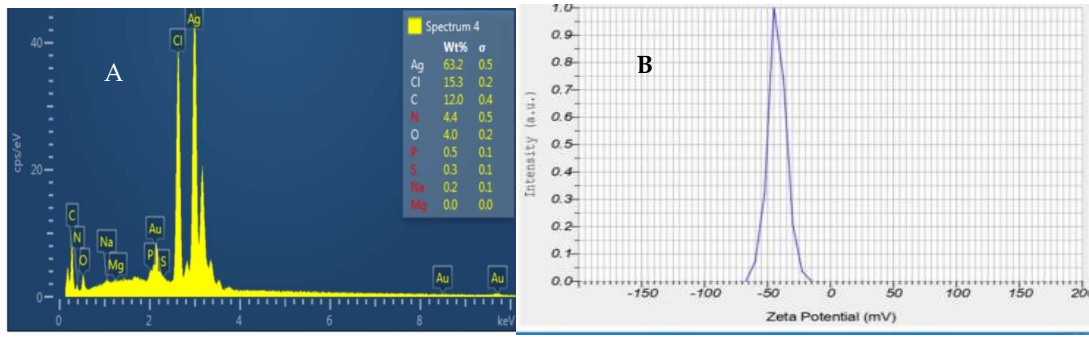

Fig. 11: Characteristics of AgNPs synthesized using *B. halotolerans* strain AhWM4. (A). EDX analysis. (B). Zeta potential value.

Energy dispersive X-ray spectroscopy (EDX) and zeta potential: The EDX analysis revealed that the elemental composition of the nanoparticles showed a significant peak at 3.0 keV, corresponding to an atomic percentage of 63.2%, indicating silver as the primary element. Additional peaks for carbon (C), oxygen (O), gold (Au), and nitrogen (N) are also observed throughout the scanning range (0–3 keV). Still, these elements are present at very low atomic percentages (Fig.11). Zeta potential analysis was conducted to evaluate the electrostatic stability of the synthesized AgNPs. The zeta potential of AgNPs was measured at -42.3 mV, indicating their superior stability Fig.11.

Dynamic light scattering (DLS): Dynamic light scattering (DLS) was employed to assess the nanoparticles' hydrodynamic diameter and aggregation in colloidal solutions. The average diameter was found to be 123 nm;

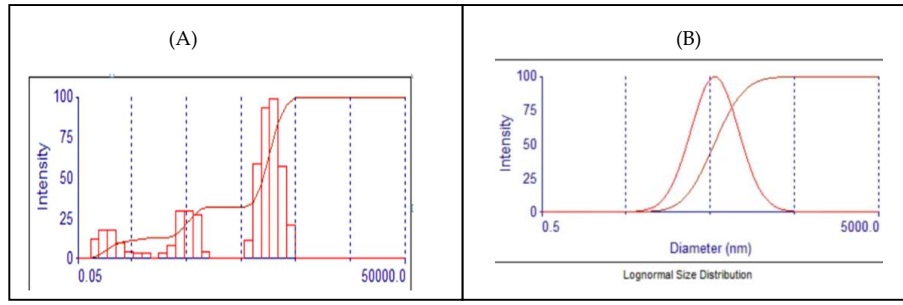

Fig. 12: Characteristic of AgNPs synthesized using the *B. halotolerans* strain AhWM4 through (A). Lognormal Distribution Multimodal Size Distribution (B). Multimodal Size Distribution.

most of the synthesized AgNPs had an effective diameter of 57.1 nm and a polydispersity index (PI) of 0.52 (Fig. 12).

DISCUSSION

The current study demonstrated a remarkable diversity of bacterial species in produced water in the Badra and Ahdab oil fields. The number of bacterial isolates in the Badra oil field was higher than in Ahdab; this may be due to differences in the physical and chemical properties of the two fields (Table 1). Other factors, such as geographical location, age of the oilfield, depth, and method of oil production, may also contribute. Al-shami et al. (2022) reported that oil reservoir environments show a great diversity of bacterial communities, influenced by a number of factors despite their harsh environmental conditions.

The results showed that the number of Gram-positive isolates in both fields was higher than that of Gram-negative isolates. This is consistent with the study of Vitaly et al. (2023). Gram-positive bacteria have a thick peptidoglycan wall, spores, enzymes, and metabolic pathways that enable them to degrade the complex hydrocarbons present in oil and use them as an energy source, giving them additional protection and a high ability to withstand harsh conditions (Huang et al. 2023). All bacterial isolates showed successful amplification of the 16S rRNA gene with fragments approximately 1,500 bp in size; these results were compatible with previous studies (Halami et al. 2024, AL-Zaidi et al. 2023, Hamzah et al. 2020b). The current study showed a clear dominance of the genus *Bacillus*, which is consistent with previous studies (Alyousif et al. 2020, Al-Tamimi et al. 2019). *Bacillus* is known for its ability to adapt to harsh conditions. Its cell wall is composed of peptidoglycan compounds, teichoic acid, and meso-diaminopimelic acid, which enhance its rigidity. Endospores play a crucial role in the persistence of this genus in these environments (Blanco Crivelli et al. 2024). These bacteria possess specific metabolic pathways that enable them to produce substances that inhibit other bacteria, giving them a competitive advantage in their living environment and making them a dominant genus in hydrocarbon-contaminated environments (Aboud et al. 2021). Through sequencing of the 16S rRNA gene, seven unique bacterial strains from the current investigation were registered in the NCBI GenBank database with specific accession codes. These bacterial isolates' DNA sequences may alter as a result of exposure to mutagens; the cause of mutation may be attributed to differences in ecological systems and exposure to mutagens, including chemicals and radiation. Several new bacterial strains isolated from Iraqi oil field environments have been reported (AL-assdy et al. 2025, Al-Shami et al. 2022, Alyousif et al. 2020).

In the present study, all bacterial isolates from the produced water of oil fields were screened for the synthesis of AgNPs. The bacterial isolates gave positive results for the nitrate reduction test and the ability to grow in the presence of 1 mM $AgNO_3$. Nitrate can be converted to nitrite by the NR enzyme, an NADH-dependent enzyme that takes up two electrons released by NADH oxidation. Released electrons can also reduce silver ions (Ag^+) to AgNPs. Metal nanotization by microbes is an essential part of geocycles and occurs as a response to heavy metal stress in harsh environments, resulting in adaptive and protective mechanisms for microbes against metal toxicity (Ghosh et al. 2021). AgNPs were synthesized using various methods, including bioreducing agents (Prodjosantoso et al. 2025). The results showed the ability of two bacterial isolate strains, *Bacillus halotolerans* strain AhWM4 and *Bacillus rugosus* strain AhWM2, to cause a colour change in the reaction mixture from light yellow to brown compared to the control. This change is an initial and visible indication of AgNP production, which occurs due to surface plasmon resonance when interacting with light. The strain *B. halotolerans* AhWM4 revealed a maximum absorption peak. Various factors, including nanoparticle size and shape, influence differences in electron density. Smaller nanoparticles may exhibit a different colour than larger ones due to variations in light interaction and electron distribution. Many previous

studies have also reported this phenomenon (Alfryyan et al. 2022, Haji et al. 2022).

UV–Vis, SEM, TEM, EDX, XRD, FTIR, zeta potential, and DLS analyses were used to characterise biosynthesised AgNPs from the bacterial strain *B. halotolerans* AhWM4. FTIR spectroscopy results showed that the bacterial supernatant contains compounds capable of reducing Ag^+ ions and acting as natural capping agents. Functional groups such as ketones, aldehydes, carboxylic acids, and amides indicate the presence of a wide range of organic compounds, including enzymes, proteins, amino acids, and carbohydrates, which may play a significant role in silver ion reduction and AgNP formation (Boldt et al. 2023, Al-Timimi et al. 2016). AgNPs exhibited a consistent crystalline structure, as shown by XRD peaks; the pattern matched the JCPDS database standard, demonstrating AgNP purity and hexagonal form (Lakhan et al. 2020). According to the Debye–Scherrer equation, broad peaks indicate small particles with an average crystallographic size of 31.33 nm. Prominent peaks indicate that bacterial extract biomolecules stabilise AgNPs. These results are similar to those reported in previous studies (Ghiuta et al. 2021, Thirumagal & Jeyakumari 2020).

The results are consistent with most previous research, which demonstrated the spherical shape of AgNPs synthesised by different *Bacillus* species, as shown by FE-SEM and TEM, with some variation in particle size (Alsamhary 2020). These differences may be due to factors such as metal ion concentration, reaction mixture temperature, duration, and pH (Marooufpour et al. 2019). AgNPs showed minimal agglomeration; this can be attributed to biomolecules that stabilise AgNPs and prevent aggregation (Khorrami et al. 2018). The EDX pattern showed a prominent silver peak with an atomic fraction of 63.2% at 3 keV, consistent with the standard silver peak associated with surface plasmon resonance. Peaks corresponding to carbon, oxygen, and nitrogen were also observed, with low atomic ratios detected in the scanning range of 0–3 keV. This indicates that biological molecules, enzymes, and proteins were associated with AgNP biosynthesis (Eid et al. 2024).

Zeta potential and DLS analyses characterise nanoparticles by particle size and surface charge. Zeta potential measurements were conducted to assess colloidal stability, with a value of −42.3 mV indicating high stability (Saied et al. 2024). Previously reported zeta potential values include −30, −34.1, −33.9, and −21.4 mV. The negative surface charge of silver nanoparticles induces electrostatic repulsion, stabilising the particles and inhibiting agglomeration (Solís-Sandí et al. 2023). The carboxyl (COOH) groups in the bacterial extract are responsible for the negative charge, as confirmed by FTIR analysis (Illanes Tormena et al. 2024). DLS measures the hydrodynamic radius of nanoparticles, which is influenced by particle size, conjugated molecules, sugars, proteins, and random or Brownian motion in solution.

CONCLUSIONS

Numerous factors influence the high diversity of bacterial communities that are found in produced water oil fields, despite their extreme environmental circumstances. Gram-positive bacteria outnumbered Gram-negative bacteria in these environments. *Bacillus* spp. was the most prevalent, with the predominant species of Bacillus cereus. The novel strain of *B. halotolerans* AhWM4 was the most effective and powerful in synthesizing AgNPs with distinct properties, an average diameter within the nanoscale range, spherical shape, and high stability in aqueous solutions, which makes it eligible for use in many medical, pharmaceutical, and environmental applications for treating various types of pollutants in the water and soil environment.

ACKNOWLEDGMENTS

The Department of Biology at the College of Science, University of Basrah, Iraq, is to be greatly thanked by the authors for providing the necessary facilities that enabled this study.

REFERENCES

Aboud, E.M., Burghal, A. and Laftah, A.H., 2021. Genetic identification of hydrocarbon-degrading bacteria isolated from oily sludge and petroleum-contaminated soil in Basrah City, Iraq. *Biodiversitas Journal of Biological Diversity*, 22(4), pp.1789–1797. [DOI]

AL-assdy, H.Q., Al-Tamimi, W.H. and Almansoory, A.F., 2024. Extracellular synthesis of iron oxide nanoparticles using several bacterial genera isolated from oil-contaminated sites in Basrah Governorate. *Egyptian Journal of Aquatic Biology and Fisheries*, 28(4), pp.1895–1914. [DOI]

AL-assdy, H.Q., Al-Tamimi, W.H. and Almansoory, A.F., 2025. Molecular detection of bacteria isolated from polluted environments and screening their ability to produce extracellular biopolymer flocculants. *Beni-Suef University Journal of Basic and Applied Sciences*, 14(1), pp.29–41. [DOI]

Alfryyan, N., Kordy, M.G., Abdel-Gabbar, M., Soliman, H.A. and Shaban, M., 2022. Characterization of biosynthesized intracellular and extracellular plasmonic silver nanoparticles using *Bacillus cereus* and their catalytic reduction of methylene blue. *Scientific Reports*, 12(1), pp.12495–12508. [DOI]

AL-Salami, R.B., Mukhaifi, E.A. and AL-Tamimi, W.H., 2024. Investigation of the effect of electric fields on bacteria isolated from skin infections. *Biodiversitas Journal of Biological Diversity*, 25(3), pp.987–995. [DOI]

Alsamhary, K.I., 2020. Eco-friendly synthesis of silver nanoparticles by *Bacillus subtilis* and their antibacterial activity. *Saudi Journal of Biological Sciences*, 27(8), pp.2185–2191. [DOI]

AL-shami, H.G.A., Al-Tamimi, W.H. and Hateet, R.R., 2022. Screening for extracellular synthesis of silver nanoparticles by bacteria isolated from Al-Halfaya oil field reservoirs in Missan Province, Iraq. *Biodiversitas Journal of Biological Diversity*, 23(7), pp.3561–3569. [DOI]

AL-Shami, H.G.A., Al-Tamimi, W.H. and Hateet, R.R., 2023. Antioxidant potential of copper oxide nanoparticles synthesized from a novel

bacterial strain. *Biodiversitas Journal of Biological Diversity*, 24(5), pp.2450–2458. [DOI]

Al-Tamimi, W.H., Lazim, S.A., Abd Al-sahib, M.A., Hameed, Z.M., Al-Amara, S.S.M., Burghal, A.A. and Al-Maqtoofi, M.Y., 2019. Improved oil recovery using biosurfactants produced by bacilli bacteria isolated from Iraqi oil reservoirs. *Pollution Research*, 38(3), pp.551–556.

Al-Timimi, I.A.J., Sermon, P.A., Burghal, A.A., Salih, A.A. and Alrubaya, I.M., 2016. Nanoengineering the antibacterial activity of biosynthesized TiO_2, Ag, and Au nanoparticles and their nanohybrids with Portobello mushroom spores. *Biosensors and Nanomedicine IX*, 9930, pp.42–54. SPIE. [DOI]

Alyousif, N., Al Luaibi, Y.Y. and Hussein, W., 2020. Distribution and molecular characterization of biosurfactant-producing bacteria. *Biodiversitas Journal of Biological Diversity*, 21(9), pp.4034–4040. [DOI]

Alyousif, N.A., Al-Tamimi, W.H. and Abd Al-Sahib, M.A., 2022. Effect of nutritional and environmental factors on biosurfactant production by *Staphylococcus epidermidis*. *Biodiversitas Journal of Biological Diversity*, 23(7), pp.3533–3538. [DOI]

AL-Zaidi, M.H.H., AL-Tamimi, W.H. and Saleh, A.A.A., 2023. Molecular determination of microbial diversity associated with vaginitis and antimicrobial sensitivity profiling. *Biodiversitas Journal of Biological Diversity*, 24(8), pp.4253–4261. [DOI]

Arshad, F., Naikoo, G.A., Hassan, I.U., Chava, S.R., El-Tanani, M., Aljabali, A.A. and Tambuwala, M.M., 2024. Bioinspired green synthesis of silver nanoparticles for medical applications. *Applied Biochemistry and Biotechnology*, 196(7), pp.3636–3669. [DOI]

Astruc, D., 2020. Introduction: Nanoparticles in catalysis. *Chemical Reviews*, 120(2), pp.461–463. [DOI]

Augustine, J.A., 2023. Degradative potential of bacteria isolated from crude oil-contaminated soil. *bioRxiv*, 2023(10), pp.1–15. [DOI]

Bharose, A.A., Hajare, S.T., G, H.P., Soni, M., Prajapati, K.K., Singh, S.C. and Upadhye, V., 2024. Bacteria-mediated green synthesis of silver nanoparticles and antifungal activity against *Aspergillus flavus*. *PLOS ONE*, 19(3), e0297870. [DOI]

Bhusal, A. and Muriana, P.M., 2021. Isolation and characterization of nitrate-reducing bacteria for the conversion of vegetable-derived nitrate to natural nitrite. *Applied Microbiology*, 1(1), pp.11–23. [DOI]

Blanco Crivelli, X., Cundon, C., Bonino, M.P., Sanin, M.S. and Bentancor, A., 2024. The complex and evolving genus *Bacillus*: A versatile bacterial powerhouse. *Bacteria*, 3(3), pp.256–270. [DOI]

Boldt, A., Walter, J., Hofbauer, F., Stetter, K., Aubel, I., Bertau, M., Jäger, C.M. and Walther, T., 2023. Cell-free synthesis of silver nanoparticles in spent media of different *Aspergillus* species. *Engineering in Life Sciences*, 23(3), e202200052. [DOI]

Burghal, A.A., Al-Tamimi, W.H. and Al-Amara, S.S.M., 2021. A novel oil-degrading bacterium *Kocuria flava* Basra AWS strain. *Pollution Research*, 40(Special Issue), pp.S200–S205.

Eid, A.M., Hassan, S.E.D., Hamza, M.F., Selim, S., Almuhayawi, M.S., Alruhaili, M.H., Tarabulsi, M.K., Nagshabandi, M.K. and Fouda, A., 2024. Photocatalytic, antimicrobial and cytotoxic efficiency of biogenic silver nanoparticles fabricated by *Bacillus amyloliquefaciens*. *Catalysts*, 14(7), pp.419–433.

Gao, Y., Wang, W., Jiang, S., Jin, Z., Guo, M., Wang, M., Li, H. and Cui, K., 2024. Response characteristics of community structure and metabolic genes of oil-recovery bacteria after targeted activation of petroleum hydrocarbon-degrading bacteria in low-permeability oil reservoirs. *ACS Omega*, 9(31), pp.33448–33458.

Ghiuta, I., Croitoru, C., Kost, J., Wenkert, R. and Munteanu, D., 2021. Bacteria-mediated synthesis of silver and silver chloride nanoparticles and their antimicrobial activity. *Applied Sciences*, 11(7), pp.3134–3146.

Ghosh, S., Ahmad, R., Banerjee, K., AlAjmi, M.F. and Rahman, S., 2021. Mechanistic aspects of microbe-mediated nanoparticle synthesis. *Frontiers in Microbiology*, 12, pp.638068–638082.

Haji, S.H., Ali, F.A. and Aka, S.T.H., 2022. Synergistic antibacterial activity of silver nanoparticles biosynthesized by carbapenem-resistant Gram-negative bacilli. *Scientific Reports*, 12(1), pp.15254–15266.

Hamzah, A., Abd-Alsahib, W. and Mahdi, S., 2020b. Isolation and identification of novel bacterial strains from different sources of the Al-Rafidiyah oil field in Iraq. *Catrina: International Journal of Environmental Sciences*, 21(1), pp.15–22.

Hamzah, A.F., Al-Mossawy, M.I., Al-Tamimi, W.H., Al-Najm, F.M. and Hameed, Z.M., 2020a. Enhancing the spontaneous imbibition process using biosurfactants produced from bacteria isolated from Al-Rafidiya oil field for improved oil recovery. Journal of Petroleum Exploration and Production Technology, 10(8), pp.3767-3777.

Huang, Y., Roseboom, W., Brul, S. and Kramer, G., 2023. Multi-omics analysis of *Bacillus subtilis* spores formed at different environmental temperatures reveals morphological and molecular differences. *bioRxiv*, 15(2), pp.1–18.

Illanes Tormena, R.P., Medeiros Salviano Santos, M.K., Oliveira da Silva, A., Félix, F.M., Chaker, J.A., Freire, D.O., Rodrigues da Silva, I.C., Moya, S.E. and Sousa, M.H., 2024. Enhancing antimicrobial activity of silver nanoparticles using *Pelargonium si[DOI]des* extract through microwave-assisted green synthesis. *RSC Advances*, 14(30), pp.22035–22043.

John, M.S., Nagoth, J.A., Ramasamy, K.P., Mancini, A., Giuli, G., Miceli, C. and Pucciarelli, S., 2022. Synthesis of bioactive silver nanoparticles using new bacterial strains from an Antarctic consortium. *Marine Drugs*, 20(9), pp.558–570.

Kadnikov, V.V., Ravin, N.V., Sokolova, D.S., Semenova, E.M., Bidzhieva, S.K., Beletsky, A.V., Ershov, A.P., Babich, T.L., Khisametdinov, M.R., Mardanov, A.V. and Nazina, T.N., 2023**.** Metagenomic and culture-based analyses of microbial communities from petroleum reservoirs with high-salinity formation water and their biotechnological potential. *Biology*, 12(10), pp.1300–1318.

Khorrami, S., Zarrabi, A., Khaleghi, M., Danaei, M. and Mozafari, M.R., 2018. Selective cytotoxicity of green-synthesized silver nanoparticles against the MCF-7 tumor cell line and their antioxidant and antimicrobial properties. *International Journal of Nanomedicine*, 13, pp.8013–8024.

Lakhan, M., Chen, R., Shar, A., Kumar, K., Chandio, M.B., Shah, A., Ahmed, M., Naich, R. and Wang, J., 2020. *Illicium verum* as a green source for silver nanoparticle synthesis and evaluation of antidiatom activity. *Sukkur IBA Journal of Emerging Technologies*, 3(1), pp.23–30.

Lee, P.Y., Costumbrado, J., Hsu, C.Y. and Kim, Y.H., 2012. Agarose gel electrophoresis for the separation of DNA fragments. *Journal of Visualized Experiments*, 62, pp.e3923–e3931.

Marooufpour, N., Alizadeh, M., Hatami, M. and Asgari Lajayer, B., 2019. Biological synthesis of nanoparticles by different bacterial groups. In: R. Prasad (ed.) *Microbial Nanobionics: Nanotechnology in the Life Sciences*. Springer, Cham, pp.1–20.

Pallavi, S.S., Rudayni, H.A., Bepari, A., Niazi, S.K. and Nayaka, S., 2022. Green synthesis of silver nanoparticles using *Streptomyces hirsutus* and their antimicrobial and anticancer activity. *Saudi Journal of Biological Sciences*, 29(1), pp.228–238.

Prodjosantoso, A.K., Nurul Hanifah, T.K., Utomo, M.P., Budimarwanti, C. and Sari, L.P., 2025. Synthesis of AgNPs/SAC using banana frond extract as a bioreducing agent and its application as a photocatalyst for methylene blue degradation. *Nature Environment and Pollution Technology*, 24(1), pp.55–66.

Rajbongshi, A. and Gogoi, S.B., 2021. A review of anaerobic microorganisms isolated from oil reservoirs. *World Journal of Microbiology and Biotechnology*, 37(7), pp.111–125.

Rose, G.K., Thakur, B., Soni, R. and Soni, S.K., 2023. Biosynthesis of silver nanoparticles using nitrate reductase from *Aspergillus terreus* and their application as a non-alcoholic disinfectant. *Journal of Biotechnology*, 373, pp.49–62.

Saied, E., Abdel-Maksoud, M.A., Alfuraydi, A.A., Kiani, B.H., Bassyouni, M., Al-Qabandi, O.A., Bougafa, F.H.E., Badawy, M.S.E.M. and Hashem, A.H., 2024. Endophytic *Aspergillus hiratsukae* mediated biosynthesis of silver nanoparticles and their antimicrobial and photocatalytic activities. *Frontiers in Microbiology*, 15, pp.1345423–1345440.

Saleh, M.N. and Alwan, S.K., 2020. Biosynthesis of silver nanoparticles from *Klebsiella pneumoniae* and their antibacterial properties. *Journal of Physics: Conference Series*, 1664(1), pp.1–15.

Singh, J., Yadav, P., Pal, A. and Mishra, V., 2020. Water pollutants: Origin and status. In: *Sensors in Water Pollutants Monitoring: Role of Materials*. Springer, Singapore, pp.5–20.

Solís-Sandí, I., Cordero-Fuentes, S., Pereira-Reyes, R., Vega-Baudrit, J.R., Batista-Menezes, D. and Montes de Oca-Vásquez, G., 2023. Optimization of biosynthesis of silver nanoparticles using bacterial extracts and evaluation of antimicrobial potential. *Biotechnology Reports*, 40, pp.e00816–e00830.

Thirumagal, N. and Jeyakumari, A.P., 2020. Structural, optical and antibacterial properties of green-synthesized silver nanoparticles using *Justicia adhatoda* leaf extract. *Journal of Cluster Science*, 31(3), pp.487–497.

Vitaly, V., Kadnikov, V.V., Ravin, N.V., Sokolova, D.S., Semenova, E.M., Bidzhieva, S.Kh., Beletsky, A.V., Ershov, A.P., Babich, T.L., Khisametdinov, M.R., Mardanov, A.V. and Nazina, T.N., 2023. Metagenomic and culture-based analyses of microbial communities from petroleum reservoirs with high-salinity formation water. *Biology*, 12(10), pp.1300–1318.

Yali, R.R., Almansoory, A.F. and Al-Tamimi, W.H., 2023. Isolation and identification of bacteria from hydrocarbon-contaminated sites for silver nanoparticle production. *Marsh Bulletin*, 18(1), pp.45–58.

Ziganshina, E.E., Mohammed, W.S. and Ziganshin, A.M., 2023. Microbial diversity of produced waters from oilfields in the Republic of Tatarstan and their participation in biocorrosion. *Applied Sciences*, 13(24), pp.12984–12998.